



## Interpreting transient carbonate compensation depth changes by marine sediment core modeling

Andy Ridgwell<sup>1</sup>

Received 26 September 2006; revised 7 July 2007; accepted 30 July 2007; published 24 October 2007.

[1] With the advent of computationally fast “intermediate complexity” models of Earth’s climate and carbon cycle the marine record can be interpreted much more directly than before. Specifically, the mechanistic simulation of deep-sea sediment cores provides an important step in bridging the model-data divide. Here I use this methodology to help interpret the excursion in carbonate compensation depth (CCD) during the Paleocene-Eocene thermal maximum that is recorded in cores recovered from Walvis Ridge in the South Atlantic. By explicitly simulating the expected geological record of a massive CO<sub>2</sub> release in an Earth system model I show how reduction in the intensity of subsurface mixing of the sediment by benthic animals substantially magnifies the recorded shoaling of the CCD. Conversely, to quantify correctly the carbon release consistent with the observed CCD changes, one must account for any bioturbational changes. A reduction in sediment mixing intensity also appears to be important to reproducing the sharpness of the contact between carbonate-rich late Paleocene sediments and the overlying early Eocene clay layer at Walvis Ridge. Assuming a relatively rapid (approximately 1 ka duration) CO<sub>2</sub> release further helps to account for some of the paleoceanographic observations. Finally, interbasin differences in bioturbational regime help resolve some of the observed disparity in carbonate preservation between Walvis Ridge and sites outside of the Atlantic, although changes in ocean ventilation and circulation are also likely to play a critical role in this.

**Citation:** Ridgwell, A. (2007), Interpreting transient carbonate compensation depth changes by marine sediment core modeling, *Paleoceanography*, 22, PA4102, doi:10.1029/2006PA001372.

### 1. Introduction

[2] Much of the available information regarding changes in climate and global carbon cycling since the late Mesozoic comes from sediment cores recovered from the ocean floor. Models of climate and/or biogeochemical cycling are becoming invaluable tools for interpreting the wealth of paleoceanographic proxies that record information about the state and operation of the Earth system. However, to assess most effectively the extent to which a simulation is consistent with observations it is important to provide model output that is as directly comparable to the data as possible. In this, it is invariably easier to work forward from a description of the key processes operating toward observations (at least, where the processes are known) than to work backward, particularly where a number of nonlinear processes all combine in determining the recorded proxy. However, while the forward modeling of proxies has become important in better understanding indicators of past climatic conditions, it has yet to become established in helping interpret the paleoceanographic record of past marine biogeochemical cycling.

[3] The composition of accumulating marine sediments was initially recorded in models as a diagnostic of the basin-

scale response of the carbonate lysocline associated with the glacial-interglacial cycles of the late Neogene [Walker and Opdyke, 1995; Munhoven and Francois, 1996]. The technique was extended to include multiple proxies, both bulk and isotopic, leading to the invention of so-called “synthetic” sediment cores. These were incorporated first in zonally averaged models of marine biogeochemical cycling [Ridgwell, 2001] and subsequently in full 3-D ocean GCMs [Heinze, 2001; Ridgwell and Hargreaves, 2007]. However, despite its obvious potential, the methodology of generating sediment cores in models has yet to be taken full advantage of. In this paper, I discuss how simulating the interaction between ocean and underlying sediments in conjunction with the generation of synthetic sediment cores can greatly help in addressing a current and significant paleoceanographic problem.

[4] The Paleocene-Eocene thermal maximum (PETM) was a transient global warming event [Kennett and Stott, 1991; Zachos et al., 2003]. Carbon isotope ( $\delta^{13}\text{C}$ ) records of carbonate and organic carbon across the PETM show a prominent negative carbon isotope excursion (CIE), widely believed to represent a massive input of carbon to the ocean and atmosphere [Dickens et al., 1995; Zachos et al., 2005]. Outstanding issues, however, include the rate of release, total amount, and source of this carbon. Several authors have proposed various carbon inputs on the basis of carbon isotope mass balance equations [Dickens et al., 1995; Kurtz et al., 2003; Svensen et al., 2004; Pagani et al., 2006]. The problem is that multiple possible combinations of carbon

<sup>1</sup>School of Geographical Sciences, University of Bristol, Bristol, UK.

release and isotopic composition exist. For instance, assuming a modern exchangeable carbon reservoir of 38000 petagrams of carbon (1 petagram carbon (Pg C) = 1 gigaton carbon (Gt C)), a global CIE of  $-2.5\%$  might be explained by a release of  $\sim 1500$  Pg C with  $\delta^{13}\text{C}$  of  $-60\%$ ,  $\sim 4500$  Pg C with a  $\delta^{13}\text{C}$  of  $-21\%$ , or a mixture of the two end-members. An analogous uncertainty crops up with respect to the last glacial transition, in that the possibility of input of light  $\delta^{13}\text{C}$  from methane hydrates means that the increase in carbon storage in the terrestrial biosphere between last glacial and Holocene cannot be unambiguously deduced from the observed change in benthic foraminiferal  $\delta^{13}\text{C}$  [Maslin and Thomas, 2003].

[5] An alternative approach to constraining the carbon release during the PETM is to analyze changes in the abundance of calcium carbonate ( $\text{CaCO}_3$ ) in deep-sea sediments [Dickens *et al.*, 1997; Dickens, 2000]. The addition of  $\text{CO}_2$  to the ocean lowers carbonate ion ( $\text{CO}_3^{2-}$ ) concentrations and with it, the stability of the  $\text{CaCO}_3$  crystal structure and thus its degree of preservation in sediments [Archer *et al.*, 1997, 1998; Ridgwell and Hargreaves, 2007]. This means that a greater proportion of the  $\text{CaCO}_3$  rain reaching the sediment surface will be dissolved, and under more extreme ocean geochemical changes when the dissolution flux exceeds the rain flux, carbonates previously preserved in the sediments will be chemically eroded. Thus a massive and relatively rapid input of carbon to the ocean would be recorded as a prominent shoaling of the depth in the ocean at which the rain rate of  $\text{CaCO}_3$  to the sediments balances the dissolution flux – known as the calcite compensation depth (CCD).

[6] Ocean Drilling Program (ODP) Leg 208 drilled a depth transect of sites on Walvis Ridge (off southwest Africa) to ascertain the CCD shoaling across the PETM [Zachos *et al.*, 2005]. As expected from box modeling [Dickens *et al.*, 1997; Dickens, 2000], carbonate dissolution occurred across the PETM. However, even the shallowest site ( $\sim 1500$  m paleodepth) showed complete loss of carbonate, and since carbonate ooze is present at the deepest site (3600 m paleodepth) prior to the event the CCD must have risen by at least 2100 m in this part of the South Atlantic. This has been interpreted as necessitating an input of  $>4500$  Pg C of carbon during the PETM [Zachos *et al.*, 2005] assuming that the observations at this site are representative globally.

[7] Although the total amount of marine carbonate that is reacted with  $\text{CO}_2$  and chemically eroded from the sediments must reflect the amount of  $\text{CO}_2$  added to the system, the relationship between  $\text{CO}_2$  addition and  $\text{CaCO}_3$  dissolution is not straightforward. One reason for this is that the reduction in  $\text{CaCO}_3$  preservation in deep-sea sediments creates a global imbalance between the rate of carbonate rock weathering on land and burial in marine sediments. When this occurs, there is a progressive increase in  $\text{CO}_3^{2-}$  concentrations in the ocean, enhancing  $\text{CaCO}_3$  preservation in the sediments until burial balances weathering once more. The timescale for the recovery of the sedimentary carbonate sink by this process is  $\sim 8.5$  ka [Ridgwell and Hargreaves, 2007]. Thus the total amount of  $\text{CaCO}_3$  that is chemically eroded from the sediments should significantly diminish as

the timescale of the  $\text{CO}_2$  release approaches or exceeds this recovery timescale. On longer timescales than this, higher rates of weathering of carbonate and silicate rocks under an enhanced greenhouse climate also become important [Berner, 1999; Ridgwell and Zeebe, 2005].

[8] The  $\text{CO}_2$  release that is consistent with an observed shift in the CCD will also be affected by any contemporaneous change in particulate rain fluxes to the sediment surface, such as resulting from greenhouse warming and increased ocean stratification [Ridgwell and Hargreaves, 2007] and by porosity changes as surface sediments become more clay rich [Archer, 1996; Zeebe and Zachos, 2007]. Any large-scale reorganization in ocean circulation that alters  $\text{CO}_3^{2-}$  gradients in the deep sea will further complicate the interpretation [Zeebe and Zachos, 2007]. For instance, during the PETM, deep-sea sediment records outside of the Atlantic such as ODP Sites 1209 and 1211 on the Shatsky Rise in the Northwest Pacific (deposited at  $\sim 2000$  and  $\sim 2500$  m paleodepth, respectively [Hancock and Dickens, 2005]) do not display such extreme carbonate dissolution [Colosimo *et al.*, 2005] nor does ODP Site 690 on Maud Rise [Röhl *et al.*, 2000]. Because of these different interacting influences on sediment composition, numerical models are required to help interpret CCD changes.

[9] In this paper I employ the “GENIE-1” Earth system model (www.genie.ac.uk) of coupled climate and ocean sediment carbon cycling [Ridgwell *et al.*, 2007a; Ridgwell and Hargreaves, 2007] to examine the response of the sediments to massive  $\text{CO}_2$  release and simulate the expected imprint on the marine geological record. I show how any change in the bioturbational mixing of the sediments adds an important new dimension to the interpretation of the evolution of the CCD associated with transient hyperthermal events such as the PETM.

## 2. GENIE-1 Earth System Model

[10] GENIE-1 is based on the fast climate model of Edwards and Marsh [2005], which features a reduced physics (frictional geostrophic) 3-D ocean circulation model, coupled to a 2-D energy-moisture balance model of the atmosphere and a dynamic-thermodynamic sea ice model. The ocean model includes a representation of marine carbon cycling, which is based on a phosphate control of biological productivity and is calibrated against observational data sets of ocean geochemistry [Ridgwell *et al.*, 2007a]. Of particular relevance to this study is the addition of a model of deep-sea sedimentary stratigraphy and preservation of biogenic carbonates delivered to the ocean floor [Ridgwell and Hargreaves, 2007], illustrated in Figure 1.

[11] I have further refined the simulation of the marine geological record in GENIE-1 as follows. First, as an alternative to the lookup table approximation of Ridgwell [2001], the full “oxic-only” carbonate diagenesis model of Archer [1991, 1996] is embedded within the deep-sea sediment module (SEDGEM). This is modified from that originally described by Archer [1991, 1996] by substituting the aqueous carbonate chemistry scheme of Ridgwell *et al.* [2007a] to calculate the dissociation constants and calcite saturation. I have also replaced the original linear-with-

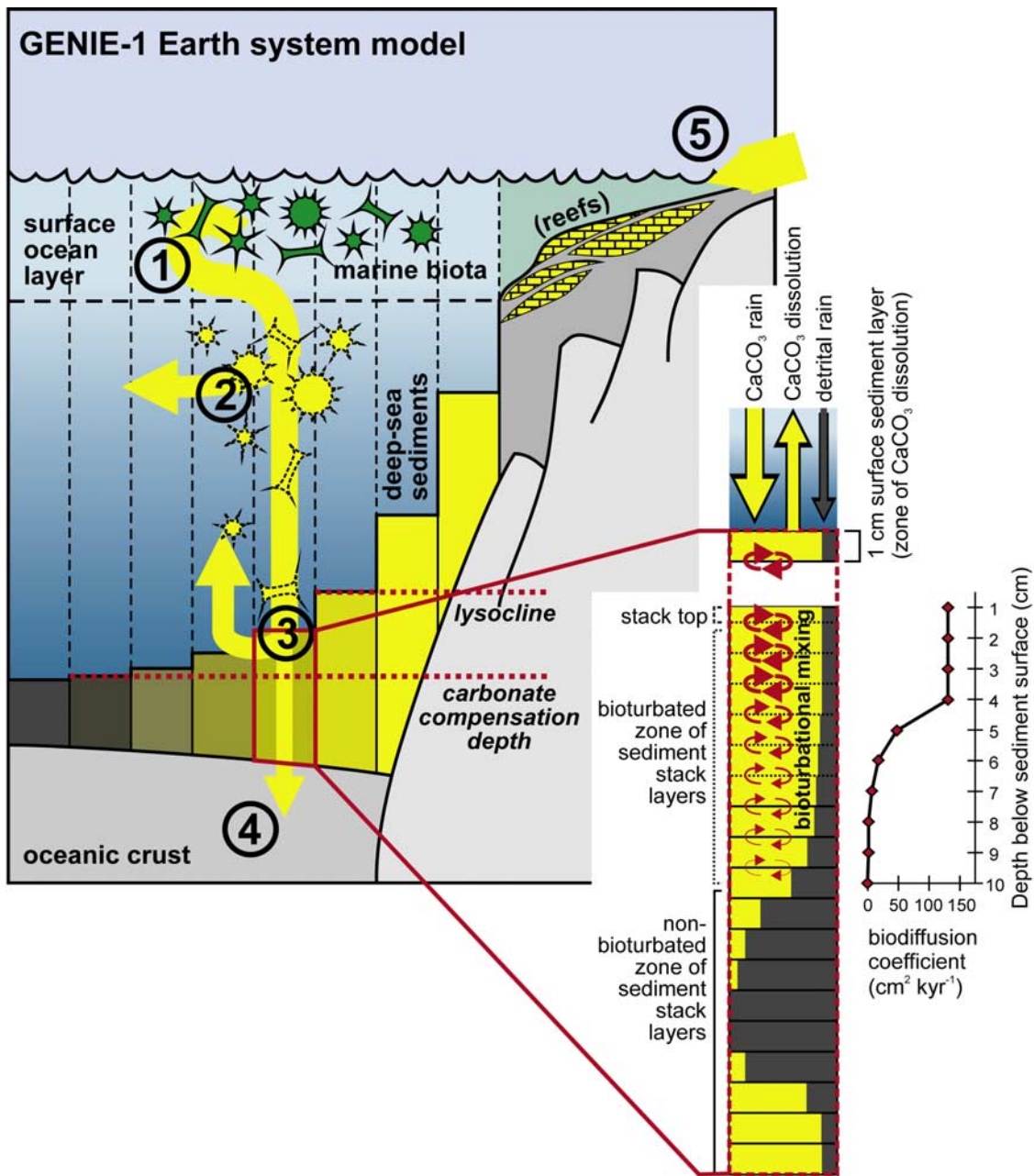


**Figure 1.** Schematic representation of the configuration of the sediment model and its relationship to marine carbonate cycling. The marine carbonate cycle in the GENIE-1 model [Ridgwell and Hargreaves, 2007] comprises five processes: (1) plankton calcification ( $\text{Ca}^{2+} + 2\text{HCO}_3^- \rightarrow \text{CaCO}_3 + \text{CO}_{2(\text{aq})} + \text{H}_2\text{O}$ ) and CaCO<sub>3</sub> export from the surface ocean, (2) dissolution of biogenic CaCO<sub>3</sub> in the water column ( $\text{CaCO}_3 + \text{CO}_{2(\text{aq})} + \text{H}_2\text{O} \rightarrow \text{Ca}^{2+} + 2\text{HCO}_3^-$ ), (3) dissolution of CaCO<sub>3</sub> within the surface sediments, (4) burial of preserved CaCO<sub>3</sub> in accumulating sediments, and (5) solute supply to the ocean from the weathering of terrestrial rocks. Not shown is the cycle of particulate organic carbon (POC), which is assumed to be completely remineralized in the water column or at the sediment surface and is not preserved and buried in the sediments. Details of the sediment module are shown expanded, highlighting the surface layer in which the net accumulation/dissolution of CaCO<sub>3</sub> is calculated, the stack of sediment storage layers underneath, and bioturbational mixing between layers. The applied bioturbation coefficient profile is shown at the right.

composition porosity scheme with that of *Zeebe and Zachos* [2007]:

$$\phi_{\infty} = \frac{\phi_{\text{det}} + f_c \cdot F}{1 + f_c \cdot F} \quad (1)$$

where  $\phi_{\infty}$  is the porosity of material substantially below (i.e., meters to tens of meters) the sediment surface,  $f_c$  is the solid fraction of carbonate material, and

$$F = \frac{\phi_{\text{CaCO}_3} - \phi_{\text{det}}}{1 - \phi_{\text{CaCO}_3}} \quad (2)$$

The end-member porosity values for pure carbonate and detrital material, which is implicitly assumed to include contributions from opal as well as dust and material from nonaeolian (e.g., continental shelf) sources, are set to:  $\phi_{\text{CaCO}_3} = 0.61$  and  $\phi_{\text{det}} = 0.88$ , respectively [Zeebe and Zachos, 2007]. The relative change of porosity with depth below surface ( $z$ , cm) in the sediments still follows *Archer* [1996]:

$$\phi_z = \phi_{\infty} + (1 - \phi_{\infty}) \cdot e^{-\frac{z}{\alpha}} \quad (3)$$

where

$$\alpha = 0.25 \cdot f_c + 3.0 \cdot (1 - f_c) \quad (4)$$

[12] Dissolution fluxes predicted by the diagenesis model are used to drive the carbonate mass balance in the surface sediment layer in SEDGEM [Ridgwell, 2001; Ridgwell and Hargreaves, 2007]. The surface layer thickness in SEDGEM is set to 1 cm and the biodiffusion coefficient over the uppermost 5 cm of the sediments, to  $150 \text{ cm}^2 \text{ ka}^{-1}$  [Archer, 1991, 1996]. Below 5 cm depth, the biodiffusion rate decreases with an  $e$ -folding length of 1 cm [Ridgwell, 2001] as shown in Figure 1. The same prescribed depth profile of mixing intensity is applied globally in the GENIE-1 model, although one might more realistically employ an explicit function of organic carbon rain rate to the sediment surface and/or ambient deep-ocean dissolved oxygen concentration [e.g., Archer *et al.*, 2002]. The porosity of the sediment stack in SEDGEM follows the same nonlinear dependence on carbonate content as the carbonate dissolution model (equation (1)), with the porosity of the surface layer calculated by integrating the porosity profile (equation (3)) over 1 cm depth, following *Archer* [1996].

[13] For recording the impact of massive CO<sub>2</sub> release in marine sediment cores I have used the modern continental and geochemical configuration of the GENIE-1 model as described by *Ridgwell and Hargreaves* [2007]. The resolution of the deep-sea sediment model grid is set at  $72 \times 72$  (Figure 2) and sediment composition is updated every 0.5 a (compared to 0.05 a for the ocean carbon cycle and an ocean circulation time step of 0.01 a). GENIE-1 is spun up for 200 ka with atmospheric CO<sub>2</sub> held constant at 278 ppm and with a constant weathering flux equivalent to  $10.0 \text{ Tmol}$

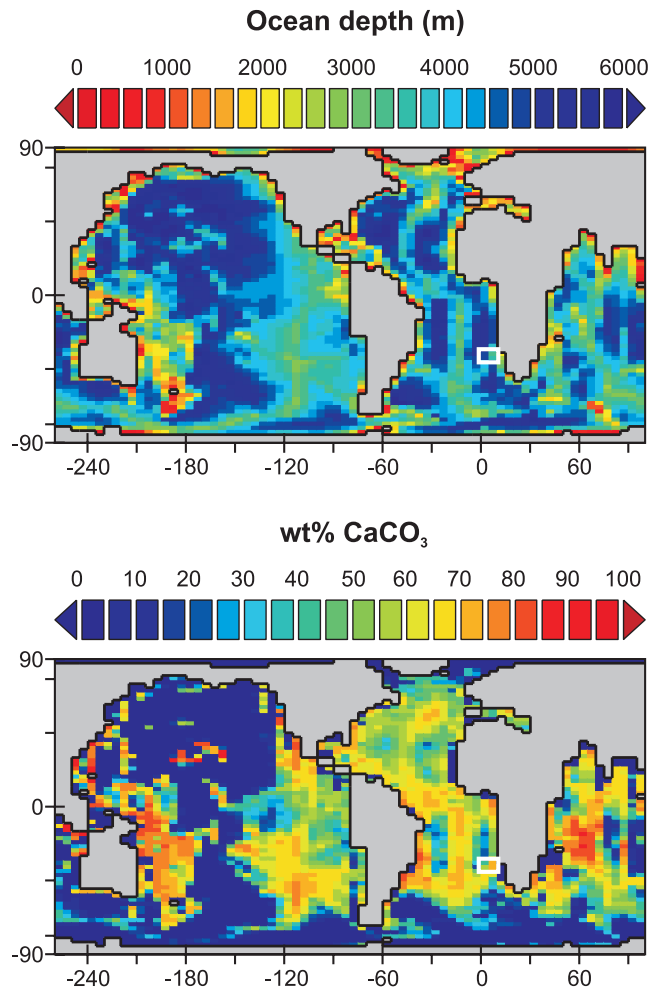


**Figure 2.** Model sediment bathymetry and predicted modern surface CaCO<sub>3</sub> distribution. (top) Assumed sediment model bathymetry on a  $72 \times 72$  (equal area) grid [Ridgwell and Hargreaves, 2007]. The white rectangle marks the (modern) Walvis Ridge location from which three synthetic sediment cores were recovered from the model. Hydrostatic pressures are prescribed in the sediment model at these locations corresponding to the estimated paleodepths of the recovered cores [Zachos *et al.*, 2005]. (bottom) Modern distribution of carbonate content of surface sediments predicted by the model [Ridgwell and Hargreaves, 2007].

CaCO<sub>3</sub> a<sup>-1</sup> ( $20.0 \text{ Tmol HCO}_3^- \text{ a}^{-1}$  or  $0.12 \text{ Pg C a}^{-1}$ ) applied to the ocean, a value diagnosed previously as balancing global carbonate burial in modern deep-sea sediments [Ridgwell and Hargreaves, 2007]. The changes made to the porosity scheme outline above in conjunction with the explicit sediment diagenesis model of *Archer* [1991, 1996] and refinements to the aqueous carbonate chemistry model discussed by *Ridgwell et al.* [2007a], together give rise to a mean global surface sedimentary composition of 34.2 wt % CaCO<sub>3</sub> compared to the 33.3 wt % reported by *Ridgwell and Hargreaves* [2007] and an observational mean of 34.8

wt %. The equilibrium distribution of surface sedimentary CaCO<sub>3</sub> content is shown in Figure 2.

### 3. Simulating the Marine Sedimentary Record of Massive CO<sub>2</sub> Release

[14] Previous analyses of the response of deep-sea sediments to massive CO<sub>2</sub> release have focused on the evolution with time of measures such as mean surface wt % CaCO<sub>3</sub> [Ridgwell and Hargreaves, 2007] or total global erodible CaCO<sub>3</sub> inventory [Archer *et al.*, 1997, 1998]. Time series of globally averaged or integrated properties are appealing because of the relative simplicity of their derivation from model output and subsequent analysis. However, paleoceanographic observations are site-specific and recorded as a function of depth in the sediments, not time. This model-data incongruence makes it difficult to interpret the data. For instance, the highest (4550 Pg C) CO<sub>2</sub> release considered by Archer *et al.* [1998] depleted all but about 5–10% of the erodable CaCO<sub>3</sub> inventory of the deep sea. However, there is no way of knowing what this means for what is observed in sediments lying at 1500 m water depth at Site 1263 in the South Atlantic, and it is therefore not safe to infer that the release must necessarily have been greater than this at the PETM [Zachos *et al.*, 2005].

[15] Analyzing how the spatial pattern of carbonate erosion evolves over time can help interpret the data. However, because of the filtering and distorting impact of the burrowing, locomotion, and feeding activities of benthic animals (“bioturbation”), the time evolution of surface sedimentary composition need not reflect what is ultimately recorded in the marine geological record as a function of depth. Exceptions to this are cores located in regions experiencing very high sedimentation rates (greater than  $\sim 10$  cm ka<sup>-1</sup>) and/or under highly oxygen limited, dysoxia or anoxic conditions. Here I show how the model-data divide can be bridged by generating sediment core records in models.

[16] The model component used to generate marine sediment records comprises a single surface layer underlain by a stack of storage layers (illustrated in Figure 1). The surface layer accounts for the gain in biogenic carbonate and noncarbonate material (detrital mineral grains plus opal) from above, loss due to in situ CaCO<sub>3</sub> dissolution, and exchange of material with the underlying sediments through bioturbational mixing. Excess material is transferred to the underlying sediment stack and provides a historical record of accumulated sediment composition as a function of depth at a resolution of 1 cm.

[17] A rather helpful advantage of the model environment over the real world is that an exact internal chronology can be devised (Figure 3). In this, carbonate newly deposited to the sediments is assigned a value equal to the current model time (as calendar years before present) divided by the mass of carbonate added [Ridgwell, 2001]. This normalization enables the effects of advection, mixing, rain input, and dissolution on sediment age to be calculated in the same way as other properties of bulk carbonate such as  $\delta^{13}\text{C}$  and  $\Delta^{14}\text{C}$ . Because it is inherently tied to the carbonate fraction, the internal numerical age scale closely parallels commonly used paleoceanographic age scales such as obtained via

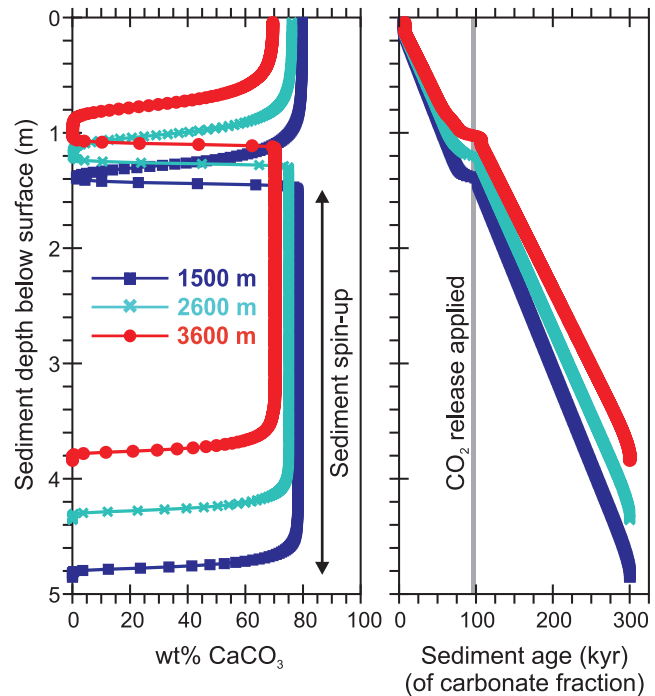


**Figure 3.** Recorded sediment properties and internal model chronology. Sediment core records are shown corresponding to a 9000 Pg C CO<sub>2</sub> release to the atmosphere over 10 ka (illustrated by the grey shading) and starting 100 ka before the end of the model run. The uppermost 5 m depth of sediments stored in the model are plotted, with sediment properties recorded at 1 cm intervals. (left) Carbonate content (wt % CaCO<sub>3</sub>) and (right) mean age of the carbonate fraction in each 1 cm interval. This internal chronology is used to plot wt % CaCO<sub>3</sub> versus age (time) (e.g., Figures 4 and 5).

orbital tuning of carbonate  $\delta^{18}\text{O}$ . The numerical age tracer even shares the same drawbacks as  $\delta^{18}\text{O}$  since no age can be calculated for a sediment layer that is completely devoid of carbonate. Although the discussion is outside the scope of this paper, it should be noted that an age scale tied to an inert, detrital fraction or to the bulk sediment as a whole will give rise to a very different chronology should any chemical erosion of carbonate from the sediments occur.

#### 3.1. Model Experimental Design

[18] Here I consider the consequences of two different CO<sub>2</sub> releases to the atmosphere – 4500 Pg C and 9000 Pg C: the first value being something like the current total recoverable conventional fossil fuel reserves [Intergovernmental Panel on Climate Change, 2001] as well as a suggested minimum estimate for the PETM [Zachos *et al.*, 2005]. I also explore the impact of releasing the carbon on two different timescales: 10 ka, reflecting previous geochemical modeling [Dickens *et al.*, 1997; Dickens, 2000], and 1 ka, which assumes a rather shorter release more comparable to the current rate of fossil fuel burn, and one more consistent with inferences made from high-resolution records from ODP Sites 690 and 1051 [Farley

and Eltgroth, 2003; Katz *et al.*, 1999; Kennett and Stott, 1991; Röhl *et al.*, 2000; Thomas *et al.*, 2002]. The rate of CO<sub>2</sub> added to the atmosphere in GENIE-1 is uniform over this interval in each case. Following CO<sub>2</sub> release, the model is run for a further 90 ka (99 ka in the case of a 1 ka duration release) to record the subsequent recovery of the Earth system. Climate in the model is allowed to respond to changes in atmospheric CO<sub>2</sub>, but terrestrial weathering is held constant. In light of the uncertainties concerning marine calcifier response to ocean acidification [e.g., Ridgwell *et al.*, 2007b], the spatial pattern of CaCO<sub>3</sub>:POC export ratio from the ocean surface is also held constant and not allowed to respond to the ensuing acidification of the ocean surface.

[19] Three cores are “recovered” [Heinze, 2001] from the model sedimentary record at the modern location of the Walvis Ridge (marked in Figure 2). To facilitate model-data comparison and make the simulations somewhat more relevant to the PETM, instead of assuming modern bathymetry everywhere, the hydrostatic pressures at the 3 adjacent sediment locations are adjusted according to the estimated 1500, 2600, and 3600 m late Paleocene paleodepths of ODP Sites 1263, 1266, and 1262, respectively [Zachos *et al.*, 2005]. However, it should be recognized that the results of the modeling cannot be related directly to the observations because the Earth system at the end of the Paleocene differed in important tectonic, climatic, and ocean geochemical characteristics compared to modern. These differences are addressed elsewhere (K. Panchuk *et al.*, Evaluating potential carbon sources for the PETM isotope excursion using an Earth system model, submitted to *Geology*, 2007, hereinafter referred to as Panchuk *et al.*, submitted manuscript, 2007).

### 3.2. Simulating the Marine Geological Record of Massive CO<sub>2</sub> Release

[20] The predicted marine record of wt % CaCO<sub>3</sub> is shown in Figure 4 for both 10 ka and 1 ka release timescales. Sediment composition is plotted as a function of bulk CaCO<sub>3</sub> age relative to the time of release using the internal carbonate-tied chronology (Figure 3) and contrasted with the independently dated Walvis Ridge observations. By making this comparison in time rather than space (depth), compaction processes [Bayer and Wetzel, 1989], which become important at the 140–336 m stratigraphic depth of the Paleocene-Eocene boundary in Walvis Ridge sediments need not be taken into account in the model. I find that 4500 Pg C, a quantity identified from previously global sediment modeling [Archer *et al.*, 1998; Zachos *et al.*, 2005], drives only a rather weak depletion of carbonate regardless of whether the release is over 1 or 10 ka. In fact, it takes an input of 9000 Pg C to create an interval of pure clay at the shallowest ocean depth of Site 1263.

### 3.3. Role of Bioturbation

[21] The burrowing, locomotion, and feeding activities of benthic animals is critical to the dynamics of the carbon cycle. In the absence of bioturbation there can be no replenishment of mineral grains of CaCO<sub>3</sub> that have been dissolved at the surface from sediments lying below and the total depth of carbonate available for reaction with CO<sub>2</sub> will

be restricted. The recovery of the system must then proceed almost solely by means of the imbalance in the sources and sinks of dissolved inorganic carbon and alkalinity induced by CO<sub>2</sub> release and reduced CaCO<sub>3</sub> preservation, and much later, through the enhancement of the weathering rates of terrestrial of carbonate and calcium silicate minerals. The upshot is that atmospheric CO<sub>2</sub> and ocean chemistry is less effectively buffered without benthic animal activity and the CO<sub>2</sub> release required in order to deplete all carbonate within a given stratigraphic interval and create a clay layer is reduced. I hypothesize that this effect bears on the interpretation of CCD changes during the PETM.

[22] As noted by Dickens [2000], there may have been a significant reduction in bioturbation throughout much of the Atlantic during the CIE. For instance, ODP Site 999 on the Kogi Rise (Caribbean Sea) contains an interval of laminated sediments corresponding to the CIE [Bralower *et al.*, 1997]. Although there is evidence of some disturbance such as the presence of clay-filled burrows in the uppermost late Paleocene ooze at Site 1262, sediments from Walvis Ridge seem to lack conspicuous evidence for having been continually and intensively bioturbationally mixed throughout the CIE.

[23] Assuming that a temporary cessation or partial suppression of bioturbation occurred in the Atlantic during the CIE but not elsewhere in the ocean, could help explain why the CCD shoaled to shallower than 1500 m at sites such as Kogi Rise and Walvis Ridge, while cores spanning the Paleocene-Eocene boundary recovered from outside of the Atlantic such as Shatsky Rise in the North West Pacific exhibit a much more muted response in CaCO<sub>3</sub> content [Bralower *et al.*, 2002; Colosimo *et al.*, 2005; Hancock and Dickens, 2005]. The lack of a pronounced change in CaCO<sub>3</sub> content and absence of a clay layer in Pacific and Indian Ocean sediments could then be partly explained as a consequence of bioturbational mixing remaining then sufficient to buffer sediment surface composition against CO<sub>2</sub> driven dissolution.

[24] I test this hypothesis by simulating a second suite of cores. On the basis that changes in lithology at Site 999 suggest a geologically rapid transition from oxic to dysoxic conditions above the Paleocene-Eocene boundary and onset of laminated sedimentation [Bralower *et al.*, 1997], I make the simplest possible assumption in the model and set the biodiffusion coefficient to zero at the start of the interval of carbon release. The same time-dependent modification is made at every sediment grid point in GENIE-1, although this is not to suggest that there is evidence for the cessation of sedimentary bioturbation everywhere during the CIE. The results are shown in Figure 5.

[25] With a long (10 ka) emissions interval all but the shallowest site now become (briefly) carbonate-free in response to the 4500 Pg C CO<sub>2</sub> release. The observed extremity of CCD shoaling is fully reproduced by 9000 Pg C, whereas with continuing bioturbation (Figure 4) a few weight percent of CaCO<sub>3</sub> persists throughout the PETM at 1500 m water depth. In the absence of bioturbation the rate of CO<sub>2</sub> input is important, and even 4500 Pg C is sufficient to drive the sediments to become carbonate-free at all depths when the release interval is 1 ka.

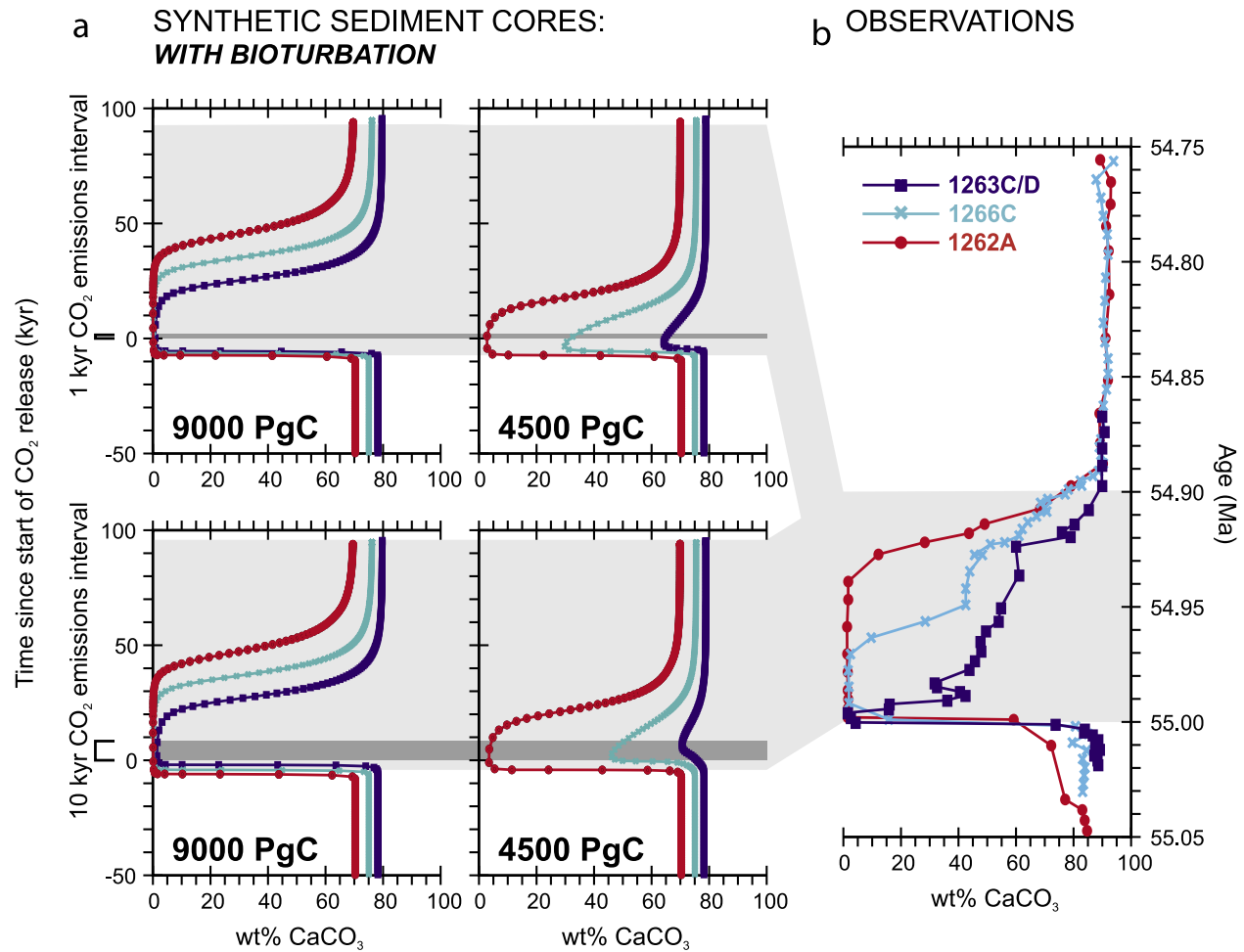


**Figure 4.** Simulated (synthetic) versus observed Walvis Ridge sediment core record of massive CO<sub>2</sub> release. (a) Modeled sediment cores for two different assumptions about the rate of CO<sub>2</sub> release: (top) 1 ka and (bottom) 10 ka and for two different emissions scenarios: (right) 4500 Pg C and (left) 9000 Pg C. The interval of CO<sub>2</sub> release is highlighted in dark grey, while the 100 ka duration of the PETM inferred from the estimated duration of carbonate depletion is highlighted in light grey. Note the creation of an offset in the apparent age of the onset of the PETM event with respect to the actual timing of CO<sub>2</sub> release. For the 9000 Pg C scenario in the model, “burn down” (chemical erosion) represents the dissolutive loss of ~5–6 ka of carbonate accumulated prior to the onset of the CIE. (b) Observed wt % CaCO<sub>3</sub> for cores: 1263C/D (1500 m paleodepth), 1266C (2600 m paleodepth), and 1262A (3600 m paleodepth) [Zachos *et al.*, 2005].

[26] Changes in bioturbational mixing also seem to be important to the rate of change of carbonate content across the Paleocene-Eocene boundary. The transition from carbonate-rich ooze to clay occurs over an interval comparable to the 1–2 cm sampling resolution in this region of the core [Zachos *et al.*, 2005]. The sharpness of the contact between high wt % CaCO<sub>3</sub> and clay-rich facies is reproduced in the simulation without bioturbation (Figure 5), whereas in the simulation with bioturbation the contact is spread over an interval of at least 5 cm (Figure 4) (the model core data points being spaced at 1 cm intervals). Furthermore, only under the assumption of a reduction in bioturbational mixing and fast CO<sub>2</sub> release can a reasonably narrow CaCO<sub>3</sub> minimum be reproduced at 1500 m depth. With continuing bioturbation mixing, a sufficient CO<sub>2</sub> release

(9000 Pg C) to create a carbonate-depleted layer at the shallowest water depth also results in a clay interval with a much longer duration than is observed.

#### 4. Discussion and Perspectives

[27] Using the GENIE-1 Earth system model I have made much better use of the available data by simulating the paleoceanographic record of massive CO<sub>2</sub> release. Under the assumption of a cessation of bioturbation and a relatively abrupt CO<sub>2</sub> release (1 ka interval) it is possible to reproduce several key features of the PETM observations at Walvis Ridge, namely: a depletion of carbonate across the range of paleodepths, the presence of a relatively narrow centimeter-scale interval of pure clay at the shallowest

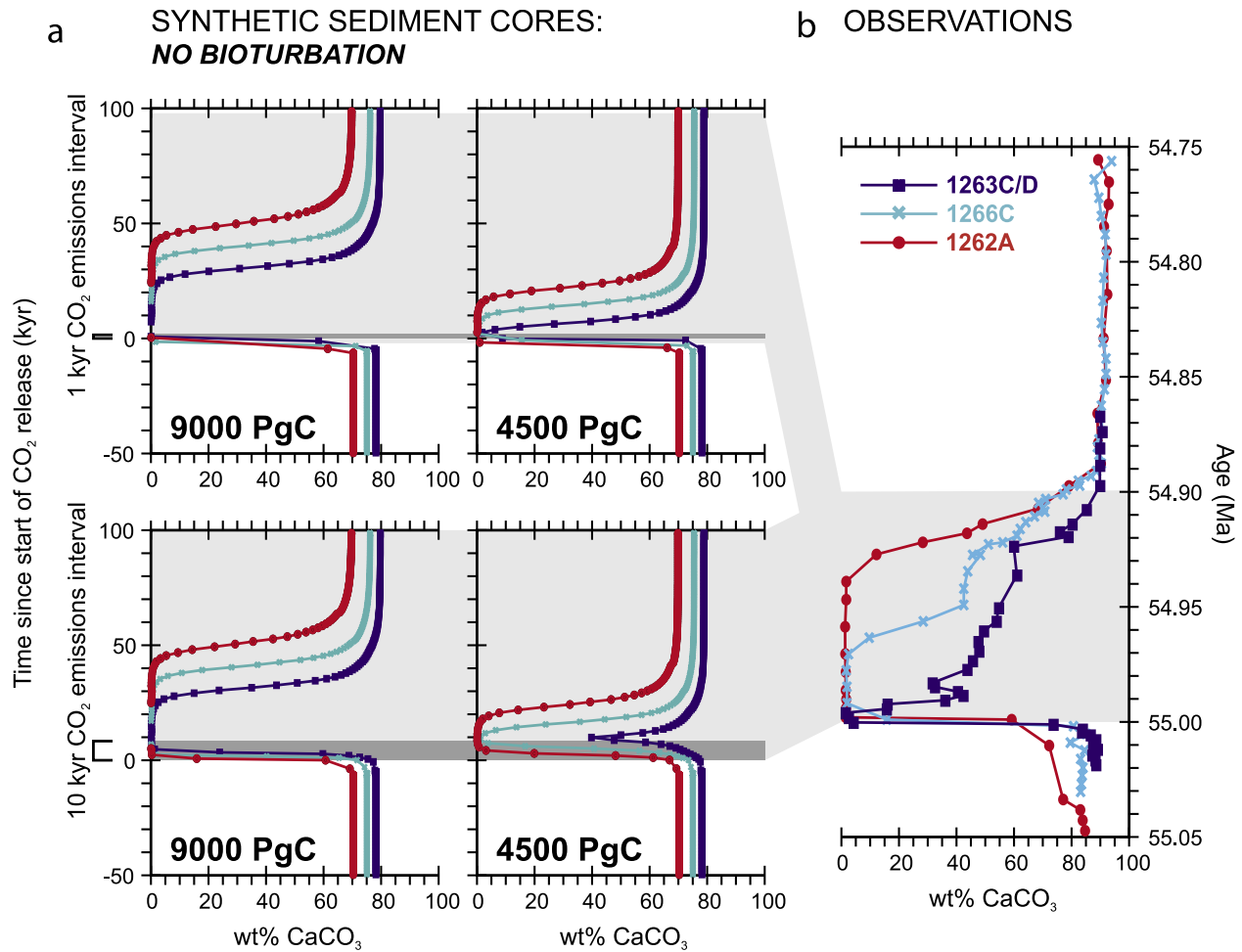


**Figure 5.** Simulated (synthetic) sediment core record in the absence of sedimentary bioturbation. All panels and model experiments are as per Figure 4, the only difference being that the experiments have been conducted with the biodiffusion coefficient in the sediment model set to zero (see section 3.3).

location (Site 1263), and a transition from late Paleocene carbonate ooze to overlying clay that takes place within 1–2 cm of core depth. A change in bioturbational regime would also help account for interbasin differences in sedimentary carbonate response. Assuming that sites outside of the Atlantic such as Shatsky Rise [Bralower *et al.*, 2002; Colosimo *et al.*, 2005; Hancock and Dickens, 2005] remained bioturbated throughout means that they would exhibit a smaller depletion of carbonate compared to at Walvis Ridge as observed. Similarly for sediments at Maud Rise – these appear to remain bioturbated throughout [Thomas *et al.*, 2002] and also retain a relatively high (>60 wt %) CaCO<sub>3</sub> composition [Röhl *et al.*, 2000].

[28] The cause of a regionally specific suppression in benthic animal activity, if correctly inferred, is not clear. The extinction event in benthic foraminifera appears globally distributed in the deep ocean and has been ascribed to the rapid warming of the deep sea at the onset of the PETM [Thomas, 2007]. That there is little evidence throughout much of the ocean for any reduction in bioturbational mixing would seem to rule out warming as a sole driver of changes in animal activity. Warming of the deep ocean also

implies a reduction in ambient dissolved oxygen concentration since the two are strongly anticorrelated via the solubility of O<sub>2</sub> in source waters. However, again, this would tend to promote a global response. I suggest that additional changes specific to the Atlantic were critical, either because of a local reduction in deepwater ventilation or perhaps additional deterioration in oxygen conditions as a result of the oxidation of a massive release of CH<sub>4</sub> [Dickens, 2000]. This is not to say that the Atlantic need have become dysoxic or anoxic. To help account for key features of the Walvis Ridge record as well as differences with observed sedimentary carbonate response elsewhere, it may be sufficient that the rate and/or maximum depth of mixing was diminished during the PETM rather than ceased entirely, *per se*.

[29] Although a fast 4500 Pg C release with no bioturbational mixing can explain the narrow clay interval at Site 1263 and sharp Paleocene-Eocene contact, the model-predicted duration of carbonate-free sediments at the deeper Sites 1262 and 1266 is rather shorter than according to the age model of Zachos *et al.* [2005] (e.g., Figure 5). To attain the inferred ~60 ka duration of clay at Site 1262 would require more than 9000 Pg C input. However, this would

make the clay layer at the shallowest location (1263) longer-lived than observations. This difficulty could be resolved if the accumulation rate during the clay rich phase is underestimated in the age model of *Zachos et al.* [2005]. However, the model-predicted thicknesses of clay (defined as <10 wt % CaCO<sub>3</sub>) in sediment cores corresponding to Sites 1263, 1266, and 1262 of: 3, 8, and 14 cm, respectively, are slightly lower than observed (5, 10, and 16 cm) [*Zachos et al.*, 2005], despite the recovered sediments having been subject to deep compaction processes not taken into account in the model. More likely then, is that the model has somewhat underpredicted the apparent duration of event, suggesting that multiple inputs spanning an interval of several tens of ka and/or a change in ocean circulation (discussed below) need to be considered.

[30] From the analysis presented here it is not possible to confidently quantify the carbon release occurring at the PETM. To refine the estimated magnitude and rate of carbon release, late Paleocene atmospheric CO<sub>2</sub> and oceanic Ca<sup>2+</sup> and Mg<sup>2+</sup> concentrations, as well as ocean circulation and sedimentation patterns all need to be accounted for within an appropriate paleogeography, discussed elsewhere (Panchuk et al., submitted manuscript, 2007). Furthermore, the apparent change in bottom water production and ventilation from a relatively proximal (Southern Ocean) source to Walvis Ridge, to a more distal (North Pacific) source [*Kennett and Stott*, 1991; *Nunes and Norris*, 2006; *Tripati and Elderfield*, 2005] will have had an impact on carbonate preservation [*Zeebe and Zachos*, 2007] and needs to be explicitly addressed. An instructive analogy can be drawn with the observed changes in carbonate deposition patterns

between the glacial and interglacials of the late Neogene, in which a circulation-driven depletion of sedimentary CaCO<sub>3</sub> in the glacial Atlantic is associated with enhanced preservation in the Pacific [*Catubig et al.*, 1998]. Part of the interbasin difference in carbonate preservation response during the CIE could then reflect a change in Atlantic ventilation – shifting the locus of preservation from Atlantic to the Pacific and Indian Oceans at the same time as CaCO<sub>3</sub> preservation everywhere is reduced in response to CO<sub>2</sub> release.

[31] Although Earth system models with an appropriate late Paleocene configuration are required to quantify the carbon release at the PETM, I have shown here that the generation of sediment cores in models of climate and marine carbon cycling provides an important interpretative advance in paleoceanography. The analysis presented here reveals a critical role for bioturbational mixing and also suggests that a CO<sub>2</sub> release interval as short as just a few thousand years may be necessary to account fully for the paleoceanographic observations at the PETM, perhaps consistent with an important role for large-scale destabilization of methane hydrates.

[32] **Acknowledgments.** A.R. wishes to express thanks to Karla Panchuk (Penn State) for discussions regarding the indicators of bioturbation, Gerald Dickens for helpful suggestions on an earlier draft of this paper, and Ellen Thomas and Ken Caldeira for constructive reviewing. This research was enabled by a University Research Fellowship from the Royal Society and NSF EAR-062871. Development of the sediment model was facilitated via Canadian Foundation for Climate and Atmospheric Sciences project grant GR-519.

## References

- Archer, D. (1991), Modeling the calcite lysocline, *J. Geophys. Res.*, *96*, 17,037–17,050.
- Archer, D. (1996), A data-driven model of the global calcite lysocline, *Global Biogeochem. Cycles*, *10*, 511–526.
- Archer, D., H. Kheshgi, and E. Maier-Reimer (1997), Multiple timescales for neutralization of fossil fuel CO<sub>2</sub>, *Geophys. Res. Lett.*, *24*, 405–408.
- Archer, D., H. Kheshgi, and E. Maier-Reimer (1998), Dynamics of fossil fuel CO<sub>2</sub> neutralization by marine CaCO<sub>3</sub>, *Global Biogeochem. Cycles*, *12*(2), 259–276.
- Archer, D. E., J. L. Morford, and S. R. Emerson (2002), A model of suboxic sedimentary diagenesis suitable for automatic tuning and gridded global domains, *Global Biogeochem. Cycles*, *16*(1), 1017, doi:10.1029/2000GB001288.
- Bayer, U., and A. Wetzel (1989), Compactional behavior of fine-grained sediments—Examples from Deep Sea Drilling Project cores, *Geol. Rundsch.*, *78*, 807–819.
- Berner, R. A. (1999), A new look at the long-term carbon cycle, *GSA Today*, *9*(11), 1–6.
- Bralower, T. J., D. J. Thomas, J. C. Zachos, M. M. Hirschmann, U. Rohl, H. Sigurdsson, E. Thomas, and D. L. Whitney (1997), High-resolution records of the late Paleocene thermal maximum and circum-Caribbean volcanism; is there a causal link?, *Geology*, *25*, 963–966.
- Bralower, T. J., I. P. Silva, and M. J. Malone (2002), New evidence for abrupt climate change in the Cretaceous and Paleogene: An Ocean Drilling Program expedition to Shatsky Rise, northwest Pacific, *GSA Today*, *12*(11), 4–10.
- Catubig, N. R., D. E. Archer, R. François, P. deMenocal, W. Howard, and E. F. Yu (1998), Global deep sea burial rate of calcium carbonate during the Last Glacial Maximum, *Paleoceanography*, *13*, 298–310.
- Colosimo, A., T. J. Bralower, and J. C. Zachos (2005), Evidence for lysocline shoaling at the Paleocene/Eocene thermal maximum on Shatsky Rise, northwest Pacific, *Proc. Ocean Drill. Program, Sci. Results*, *198*, 1–36.
- Dickens, G. R. (2000), Methane oxidation during the late Palaeocene thermal maximum, *Bull. Soc. Geol. Fr.*, *171*, 37–49.
- Dickens, G. R., J. R. O'Neil, D. K. Rea, and R. M. Owen (1995), Dissociation of oceanic methane hydrate as a cause of the carbon isotope excursion at the end of the Paleocene, *Paleoceanography*, *10*, 965–971.
- Dickens, G. R., M. M. Castillo, and J. C. G. Walker (1997), A blast of gas in the latest Paleocene; simulating first-order effects of massive dissociation of oceanic methane hydrate, *Geology*, *25*, 259–262.
- Edwards, N. R., and R. Marsh (2005), Uncertainties due to transport-parameter sensitivity in an efficient 3-D ocean-climate model, *Clim. Dyn.*, *24*, 415–433.
- Farley, K. A., and S. F. Eltgroth (2003), An alternative age model for the Paleocene-Eocene thermal maximum using extraterrestrial <sup>3</sup>He, *Earth Planet. Sci. Lett.*, *208*, 135–148.
- Hancock, H. J. L., and G. R. Dickens (2005), Carbonate dissolution episodes in Paleocene and Eocene sediment, Shatsky Rise, west-central Pacific [online], *Proc. Ocean Drill. Program Sci. Results*, *198*, 24 pp. (Available at [http://www-odp.tamu.edu/publications/198\\_SR/116/116.htm](http://www-odp.tamu.edu/publications/198_SR/116/116.htm))
- Heinze, C. (2001), Towards the time dependent modeling of sediment core data on a global basis, *Geophys. Res. Lett.*, *28*, 4211–4214.
- Intergovernmental Panel on Climate Change (2001), *Climate Change 2001: Mitigation*, edited by B. Metz et al., Cambridge Univ. Press, Cambridge, U. K.
- Katz, M. E., D. K. Pak, G. R. Dickens, and K. G. Miller (1999), The source and fate of massive carbon input during the latest Paleocene thermal maximum, *Science*, *286*, 1531–1533.
- Kennett, J. P., and L. D. Stott (1991), Abrupt deep-sea warming, paleoceanographic changes and benthic extinctions at the end of the Paleocene, *Nature*, *353*, 225–229.
- Kurtz, A. C., L. R. Kump, M. A. Arthur, J. C. Zachos, and A. Paytan (2003), Early Cenozoic decoupling of the global carbon and sulfur cycles, *Paleoceanography*, *18*(4), 1090, doi:10.1029/2003PA000908.

- Maslin, M. A., and E. Thomas (2003), Balancing the deglacial global carbon budget: The hydrate factor, *Quat. Sci. Rev.*, *22*, 1729–1736.
- Munhoven, G., and L. M. Francois (1996), Glacial-interglacial variability of atmospheric CO<sub>2</sub> due to changing continental silicate rock weathering: A model study, *J. Geophys. Res.*, *101*, 21,423–21,437.
- Nunes, F., and R. D. Norris (2006), Abrupt reversal ocean overturning during the Palaeocene-Eocene warm period, *Nature*, *439*, 60–64.
- Pagani, M., N. Pedentchouk, M. Huber, A. Sluijs, S. Schouten, H. Brinkhuis, J. S. Sinninghe Damsté, and G. R. Dickens (2006), Arctic hydrology during global warming at the Palaeocene/Eocene thermal maximum, *Nature*, *442*, 671–675.
- Ridgwell, A. J. (2001), Glacial-interglacial perturbations in the global carbon cycle, Ph.D. thesis, Univ. of East Anglia at Norwich, Norwich, U. K.
- Ridgwell, A., and J. C. Hargreaves (2007), Regulation of atmospheric CO<sub>2</sub> by deep-sea sediments in an Earth system model, *Global Biogeochem. Cycles*, *21*, GB2008, doi:10.1029/2006GB002764.
- Ridgwell, A., and R. E. Zeebe (2005), The role of the global carbonate cycle in the regulation and evolution of the Earth system, *Earth Planet. Sci. Lett.*, *234*, 299–315.
- Ridgwell, A., J. Hargreaves, N. Edwards, J. Annan, T. Lenton, R. Marsh, A. Yool, and A. Watson (2007a), Marine geochemical data assimilation in an efficient Earth system model of global biogeochemical cycling, *Biogeosciences*, *4*, 87–104.
- Ridgwell, A., I. Zondervan, J. C. Hargreaves, J. Bijma, and T. M. Lenton (2007b), Significant long-term increase of fossil fuel CO<sub>2</sub> uptake from reduced marine calcification, *Biogeosciences*, *4*, 481–492.
- Röhl, U., T. J. Bralower, R. D. Norris, and G. Wefer (2000), New chronology for the late Paleocene thermal maximum and its environmental implications, *Geology*, *28*, 927–930.
- Svensen, H., S. Planke, A. Malthes-Sorensen, B. Jamtveit, R. Myklebust, T. Rasmussen Eidem, and S. S. Rey (2004), Release of methane from a volcanic basin as a mechanism for initial Eocene global warming, *Nature*, *429*, 542–545.
- Thomas, D. J., J. C. Zachos, T. J. Bralower, E. Thomas, and S. Bohaty (2002), Warming the fuel for the fire: Evidence for the thermal dissociation of methane hydrate during the Paleocene-Eocene thermal maximum, *Geology*, *30*, 1067–1070.
- Thomas, E. (2007), Cenozoic mass extinctions in the deep sea: What disturbs the largest habitat on Earth?, in *Large Ecosystem Perturbations: Causes and Consequences*, edited by S. Monechi, R. Coccioni, and M. Rampino, *Spec. Pap. Geol. Soc. Am.*, *424*, 1–23, doi:10.1030/2007.2424(01).
- Tripati, A., and H. Elderfield (2005), Deep-sea temperature and circulation changes at the Paleocene-Eocene thermal maximum, *Science*, *308*, 1894–1898.
- Walker, J. C. G., and B. C. Opdyke (1995), Influence of variable rates of netitic carbonate deposition on atmospheric carbon dioxide and pelagic sediments, *Paleoceanography*, *10*, 415–427.
- Zachos, J. C., M. W. Wara, S. Bohaty, M. L. Delaney, M. R. Petrizzo, A. Brill, T. J. Bralower, and I. Premoli-Silva (2003), A transient rise in tropical sea surface temperature during the Paleocene-Eocene thermal maximum, *Science*, *302*, 1551–1554.
- Zachos, J. C., et al. (2005), Rapid acidification of the ocean during the Paleocene-Eocene thermal maximum, *Science*, *308*, 1611–1615.
- Zeebe, R. E., and J. C. Zachos (2007), Reversed deep-sea carbonate ion basin gradient during Paleocene-Eocene thermal maximum, *Paleoceanography*, *22*, PA3201, doi:10.1029/2006PA001395.

---

A. Ridgwell, School of Geographical Sciences, University of Bristol, University Road, Bristol BS8 1SS, UK. (andy@seao2.org)